Proc. Natl. Acad. Sci. USA
Vol. 96, pp. 8120–8125, July 1999
Medical Sciences

Megakaryocyte hyperplasia and enhanced agonist-induced platelet activation in vasodilator-stimulated phosphoprotein knockout mice

WOLFGANG HAUSER*, KLAUS-PETER KNOBELOCH†, MARTIN EIGENTHALER*, STEPAN GAMBARYAN*‡, VEIT KRENN§, JÖRG GEIGER*, MARGARITA GLAZOVA*‡, ELVIRA ROHDE†, IVAN HORAK†, ULRICH WALTER*¶, AND MICHAEL ZIMMER*

*Institut für Klinische Biochemie und Pathobiochemie und §Pathologisches Institut der Universität Würzburg, Josef-Schneider Strasse 2, 97080 Würzburg, Germany; and †Forschungsinstitut für Molekulare Pharmakologie, Abteilung Molekulare Genetik, Krahmerstrasse 6, 12207 Berlin, Germany

Communicated by David L. Garbers, University of Texas Southwestern Medical Center, Dallas, TX, March 10, 1999 (received for review November 15, 1998)

ABSTRACT **Vasodilator-stimulated phosphoprotein (VASP), a substrate of cAMP- and cGMP-dependent protein kinases, is associated with focal adhesions, cell–cell contacts, microfilaments, and highly dynamic membrane regions. VASP, which is expressed in most cell types and in particularly high levels in human platelets, binds to profilin, zyxin, vinculin, F-actin, and the *Listeria monocytogenes* surface protein ActA. VASP is a member of the enabled (Ena)/VASP protein family and is thought to be involved in actin filament formation and integrin $\alpha_{IIb}\beta_3$ inhibition in human platelets. To gain further insight into the *in vivo* function of this protein, VASP-deficient mice were generated by homologous recombination. VASP−/− mice demonstrated hyperplasia of megakaryocytes in bone marrow and spleen but exhibited no other macroscopic or microscopic abnormalities. Activation of platelets with thrombin induced a more than 2-fold higher surface expression of P-selectin and fibrinogen binding in VASP-deficient platelets in comparison to wild type. These data support the concept that VASP is a negative modulator of platelet and integrin $\alpha_{IIb}\beta_3$ activation. Although the limited phenotypic differences between wild-type and VASP−/− mice suggested functional compensation of VASP by members of the Ena/VASP family, alterations in the expression levels of mammalian enabled (Mena) and Ena-VASP-like (Evl) protein were not detected. VASP-deficient mice may provide an interesting model system for diseases in which enhanced platelet activation plays a major role.**

Vasodilator-stimulated phosphoprotein (VASP) initially was discovered and characterized as a prominent substrate for both cGMP-dependent protein kinases (cGKs) and cAMP-dependent protein kinases (cAKs) in human platelets (1, 2). VASP is phosphorylated *in vitro* and in intact human platelets at serine-157, serine-239, and threonine-278 by both cAK and cGK, and it is *in vitro* and in intact human platelet dephosphorylated by protein phosphatases I and II with overlapping selectivity (3–7). Phosphorylation of serine-157, the site preferred by cAK, leads to a shift in the apparent molecular mass of VASP in SDS/PAGE from 46 kDa to 50 kDa (5, 6). VASP phosphorylation in response to cyclic nucleotide-regulating vasodilators (i.e., cAMP-elevating prostaglandins and cGMP-elevating NO donors) closely correlates with platelet inhibition and in particular with the inhibition of fibrinogen binding to the human platelet integrin $\alpha_{IIb}\beta_3$ (3, 8). In platelets, smooth muscle cells, endothelial cells, and fibroblasts, VASP has been found to be associated with focal adhesions, stress fibers, cell–cell contacts, and highly dynamic membrane regions (9, 10). VASP is the founding member of a family of proline-rich proteins, designated the Ena/VASP protein family (11–14). In addition to VASP, this family comprises *Drosophila* Enabled (Ena), which is a substrate of the Abelson tyrosine kinase (Abl) and is genetically linked to the Abl signaling pathway (12), the mammalian Ena homolog Mena, and the Ena-VASP-like protein Evl (14). These proteins share highly homologous N-terminal and C-terminal domains (Ena-VASP homology domains 1 and 2, designated EVH1 and EVH2), and proline-rich central domains (10–14). VASP, Mena, and Ena have been shown to colocalize with and directly bind to profilin (14–16). They also bind to zyxin (14, 15, 17) and to the *Listeria monocytogenes* surface protein ActA (14, 18, 19) that is essential for the actin polymerization-based intracellular motility of this pathogen. Further, VASP is a binding partner for the focal adhesion and cell–cell contact protein vinculin *in vitro* and colocalizes with vinculin in focal contacts of living cells (20, 21). Binding of VASP and Mena to zyxin, ActA, and vinculin is mediated by interactions of the EVH1 domains with FP_4 motifs present in the respective binding partners (14, 18, 19), whereas the tandemly repeated GP_5 motifs in the central proline-rich region of VASP are involved in binding to profilin (16, 22). Direct evidence for functional homologies of the members of the Ena/VASP family stems from the observation that VASP can substitute for a complete loss of Ena in *Drosophila* when expressed via the UAS/GAL4 binary expression system (15). Ena null mutants (which die early during development) that express human VASP show similar fertility and viability compared with mutants rescued with the Ena wild-type transgene.

So far, VASP is the most extensively studied member of the Ena/VASP family. Functional evidence indicates that it is a crucial factor involved in the enhancement of spatially confined actin filament formation (17, 18, 23, 24). In human platelets, VASP appears to be involved in the inhibition of agonist-induced integrin $\alpha_{IIb}\beta_3$ activation (8, 25). Although the precise mechanisms are not well defined, the microfilament system is an essential component in integrin activation (25), and VASP might be a linking factor. To gain further insight into VASP function, we performed gene targeting in mouse embryonic stem cells to generate VASP-deficient mice. Here we report that VASP-deficient mice exhibit a very specific phenotype of megakaryocyte hyperplasia and enhanced agonist-induced activation of P-selectin expression and fibrinogen binding to the integrin $\alpha_{IIb}\beta_3$

The publication costs of this article were defrayed in part by page charge payment. This article must therefore be hereby marked "*advertisement*" in accordance with 18 U.S.C. §1734 solely to indicate this fact.

PNAS is available online at www.pnas.org.

Abbreviations: VASP, vasodilator-stimulated phosphoprotein; Ena, enabled; Mena, mammalian enabled; cGK, cGMP-dependent protein kinase; Evl, Ena-VASP-like; EVH, Ena-VASP homology; cGKI, cGMP-dependent protein kinase type I.

‡Permanent address: Sechenov Institute of Evolutionary Physiology and Biochemistry, Russian Academy of Sciences, Thozez pz. 44, St. Petersburg 194223, Russia.

¶To whom reprint requests should be addressed. e-mail: uwalter@klinbiochem.uni-wuerzburg.de.

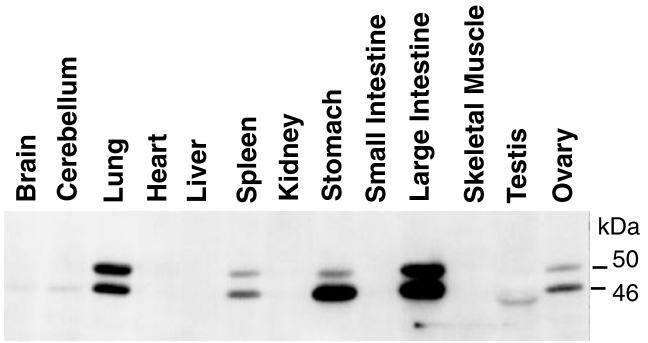

FIG. 1. Analysis of VASP expression in wild-type mice. Cell homogenates (30 μg protein per lane) were probed with an affinity-purified VASP polyclonal antibody. Equal protein loading was controlled by Ponceau staining. VASP appears as a doublet of 46 kDa and 50 kDa representing the serine-157 dephosphorylated and phosphorylated protein states, respectively. Longer exposure of this immunoblot also demonstrated VASP expression in brain, heart, kidney, and small intestine.

in platelets, but are otherwise viable, fertile, and macroscopically indistinguishable from wild-type mice.

MATERIALS AND METHODS

Generation of VASP−/− Mice. A cosmid containing the complete murine *VASP* gene was isolated from a 129Sv genomic library (13). For construction of the targeting vector the herpes simplex virus thymidine kinase (HSV-tk) cassette was cloned into the *Eco*RI–*Sal*I sites in pUC18. From this construct an *Eco*RI–*Nde*I fragment including the HSV-tk cassette was excised and used to replace the corresponding region in pUC19, leaving the multiple cloning site of pUC19 intact. A 2.2-kb *Sac*I genomic fragment from intron 3 of the *VASP* gene was cloned into the pUC19tk vector, resulting in a reverse orientation of the *tk* gene with respect to the *VASP* gene. In a second step, a 7-kb genomic *Kpn*I–*Nhe*I fragment spanning exons 5–13 was inserted in the *Kpn*I–*Xba*I sites. Digestion of this construct with *Kpn*I and *Xho*I deleted a 2.8-kb fragment including exons 5–11 of the *VASP* gene, which was replaced by a PGK-neo cassette in antisense orientation (see Fig. 3). After linearization with *Sal*I, the targeting vector (p19TV) was electroporated into embryonic stem cells derived from 129Sv/ola mice. The clones were grown under double selection as described (26). DNA from double-resistant clones was digested with *Xho*I and probed with the 303-bp *Ngo*MI/*Bsm*BI fragment of the human *VASP* cDNA (11), comprising exons 2 and 3. This probe detected a 6.5-kb wild-type *Xho*I fragment, and homologous recombination generated a 4.9-kb recombinant *Xho*I fragment. Southern blot results were confirmed by PCR using primers located in exon 3 (5′-TGGGCTAGCAGGTGGGATTGTGTTGGGG-3′) and in the PGK-neo cassette (5′-CATCGCCTTCTATCGCCTTCT-3′). After expansion, one mutant clone was injected into C57BL/6 blastocysts. The resulting chimeras were bred with C57BL/6 mice, and germ-line transmission was determined by Southern blot and PCR analysis.

DNA, RNA, and Protein Analysis. DNA and RNA was isolated according to standard methods (27). Southern blots and hybridizations were performed as described by Church and Gilbert (28). Poly(A)$^+$ RNA was purified by using the Olitex mRNA Kit (Qiagen). Northern blots were hybridized with full-length human *VASP* (11) or mouse *Evl* cDNA (14) probes. Tissues used for Western blots were dissected from nembutal-anesthesized, saline-perfused mice and were homogenized in PBS containing protease inhibitors (5 μg/ml of leupeptin, 1.5 mM benzamidine, 200 units/ml of aprotinin, 2 μg/ml of pepstatin A, 10 μg/ml of

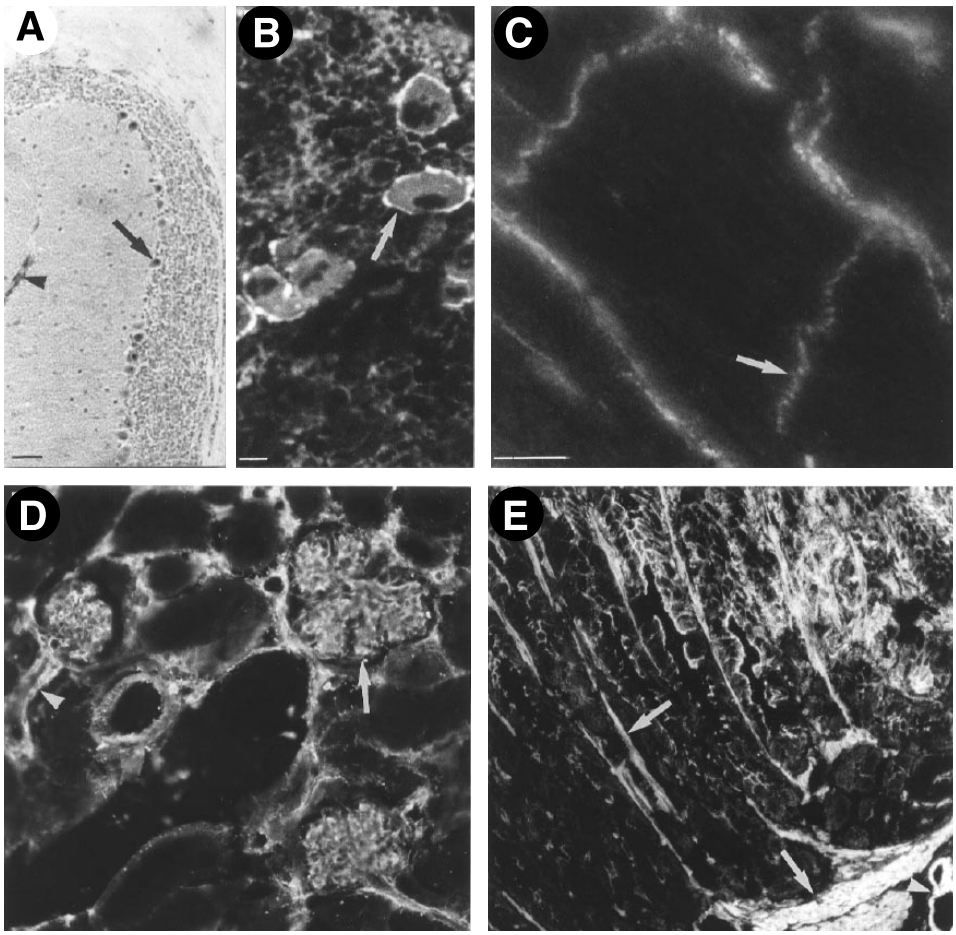

FIG. 2. Distribution of VASP in mouse tissues. In cerebellum (*A*) VASP is expressed in Purkinje cells (arrow). In spleen (*B*) the highest level is detected in megakaryocytes (arrow). In cardiomyocytes (*C*) VASP is localized in intercalated discs (arrow), in kidney (*D*) in glomerular mesangial cells, and in stomach (*E*) in smooth muscle cells. In all tissues shown, high levels of VASP also were detected in vascular smooth muscle cells (arrowheads). (Bar corresponds to 50 μm in *A*, *D,* and *E*, and 10 μm in *B* and *C*.)

PMSF, and 1 mM EDTA). Platelets were isolated from whole blood. Protein content was measured by Bio-Rad Bradford assay. Tissue homogenates or platelets were mixed with an equal volume SDS-containing stop solution and directly loaded onto 8% SDS-polyacrylamide gels (15% gel for profilin). The gels were blotted onto nitrocellulose and labeled with antisera or mAbs, followed by peroxidase labeled anti-rabbit or anti-mouse antibody and ECL detection (Amersham Pharmacia). Polyclonal antisera were affinity-purified VASP (1:500) (9), cGMP-dependent protein kinase type I (cGKI) (1:2,000) (29), profilin (1:4,000, Immunoglobe, Grassostheim, Germany), and zyxin (1:5,000) (17). mAbs were vinculin (1:4,000; Sigma) and Mena (1:250; Transduction Laboratories, Lexington, KY).

Histological Analysis. Pairs of wild-type and VASP−/− mice from three independent litters were analyzed. Tissue samples were fixed in 4% formalin, and bones were decalcified in 10 mM EDTA for 4 days and embedded in paraffin. Tissue sections (4 μm) were stained in Giemsa, hematoxylin/eosin Gomöry, and periodic acid/Schiff reagent by using standard protocols. Bone marrow was analyzed in a similar method as stained tissue sections. The quantity of megakaryocytes was semiquantitatively ascertained by scoring 10 high-power fields on three different sections. The ANOVA test was used for statistical analysis.

Immunocytochemistry. Tissues from PBS/parafomaldehyde (4%)-perfused mice were prepared and analyzed as described (29) by using affinity-purified polyclonal VASP antibodies (9).

Flow Cytometry Analysis of Platelet-Rich Plasma. Acid-citric acid-dextrose anticoagulated mouse blood was diluted with an equal volume of PBS (containing 0.5% BSA) and centrifuged for 2 min at 350 *g* in a microcentrifuge. Platelet-rich plasma was removed, further diluted with PBS (containing 0.5% BSA, 5.5 mM glucose, 1 mM $CaCl_2$, and 1 mM $MgCl_2$), and both 1.5 μg biotinylated anti-CD62P (P-selectin) antibody (PharMingen) and 3 μg FITC-labeled anti-fibrinogen antibody (WAK Chemie, Bad Soden, Germany) were added to each sample before stimulation with 0.5 units/ml of thrombin at 37°C. Aliquots of the cell suspension were removed at given time points, reactions were stopped by addition of 1% (final concentration) of methanol-free formaldehyde, and samples were fixed for 8 min at room temperature. Platelets were pelleted for 1 min at 2,000 *g*, resuspended in 50 μl of PBS with 2 μl streptavidin-PerCP (Becton Dickinson), incubated for 20 min at room temperature in the dark, and diluted with PBS before flow cytometry analysis using a Becton Dickinson FACSCalibur was performed. The number of fibrinogen receptors was determined by using FITC-conjugated anti-mouse CD41 (PharMingen) in the absence of thrombin stimulation.

RESULTS

Expression of Mouse VASP. Sequencing and structural analysis of the human and mouse *VASP* genes previously had revealed a housekeeping-like promoter (13), suggesting a ubiquituous expression of the VASP protein. In Western blot analysis a VASP antiserum detected two bands with apparent molecular masses of 46 kDa and 50 kDa in selected mouse tissues, except for testis (Figs. 1 and 2). The signals represented differentially phosphorylated forms of VASP, the 50-kDa band resulting from a shift in electrophoretic mobility because of the phosphorylation of Ser-157 (2, 5). Only in testis did the VASP antiserum detect a band slightly smaller than 46 kDa that has not been further characterized. The amount of VASP was markedly different in various mouse tissues and cells (Figs. 1 and 2). Highest expression was observed in platelets, but VASP was also abundant in lung, stomach, large intestine, and vascular smooth musle. In brain, heart, kidney, and small intestine VASP expression was significantly less, but clearly detectable after a longer exposure of the Western blot shown in Fig. 1. Immunhistochemistry showed that in these tissues VASP was expressed only in specific cells like cerebellar Purkinje cells, megakaryoctes, cardiac myocytes, and glomerular mesangial cells (Fig. 3). VASP expression was not detectable in liver and in skeletal muscle by either method.

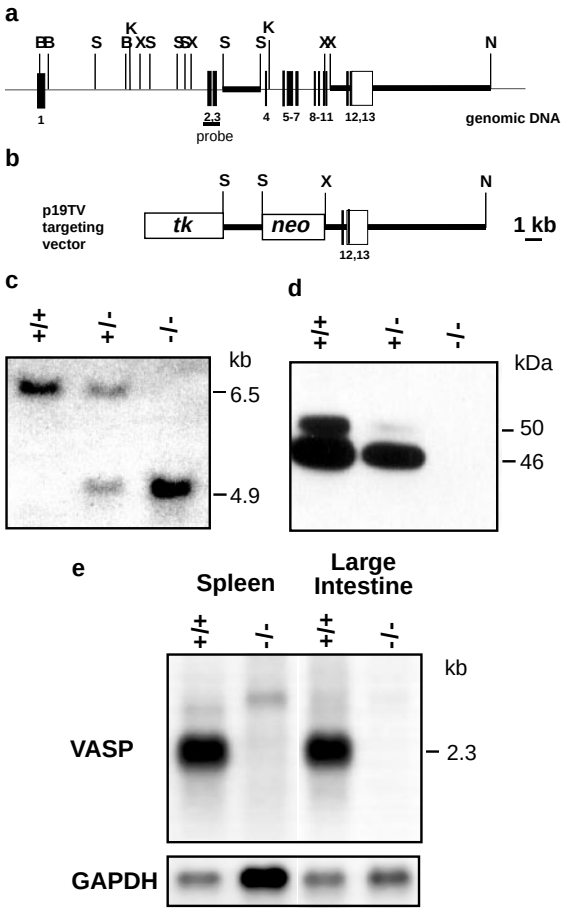

FIG. 3. Targeted disruption of the *VASP* gene. (*a*) Organization of the wild-type *VASP* gene and positions of relevant restriction sites (B, *Bam*HI; K, *Kpn*I; N, *Nhe*I; S, *Sac*I; X, *Xho*I). Closed bars represent VASP coding exons, the open box indicates the 3′ untranslated region. Exons are numbered underneath. Thick lines represent the genomic fragments that were subcloned for construction of the targeting vector. The probe for Southern blot hybridization spans exons 2 and 3. (*b*) Targeting vector. The neomycin resistence gene (*neo*) was introduced in an antisense orientation with respect to the *VASP* gene. *tk,* thymidine kinase gene. (*c*) Southern blot analysis using DNA extracted from tail biopsies of wild-type (+/+), heterozygous (+/−), and homozygous (−/−) mice. DNA was digested with *Xho*I. Hybridization with the probe encompassing exons 2 and 3 yielded bands of 6.5 kb (wild-type allele) and 4.9 kb (mutant allele) in size. (*d*) Western blot analysis of VASP expression in platelets derived from wild-type, heterozygous, and mutant animals. The 46-kDa and 50-kDa proteins represent the serine-157 dephospho- and phospho-forms of VASP, respectively. (*e*) Northern blot analysis of poly(A)$^+$ RNA from spleen and large intestine, wild-type and VASP−/− mice. The blots were hybridized with a human *VASP* full-length cDNA probe. For comparison of RNA amounts loaded the blots were hybridized with a mouse glyceraldehyde-3-phosphate dehydrogenase (GAPDH) cDNA probe.

Generation of VASP-Deficient Mice. The *VASP* gene was interrupted by targeted integration of a neomycin-resistance cassette (PGK-neo) in intron 3, with concurrent deletion of exons 4–11. Homologous recombination resulted in a mutant gene that was lacking the exons encoding the proline-rich central domain and the proximal part of the EVH2 domain (11). Synthesis of the C-terminal 31 aa that are encoded by exons 12 and 13 also was excluded, because a putative splicing event that might join exon 3 with exon 12 would result in a frame shift. However, because the *VASP* gene was interrupted only after exon 3, expression of the N-terminal 114 aa, which basically represent the VASP EVH1 domain, theoretically could not be excluded. Immunoblot analysis of platelet protein with affinity-purified VASP antibodies (as well as with an antiserum specifically raised against the 114-residue N-terminal VASP fragment) showed a significant reduction of

VASP in heterozygous animals compared with wild type and failed to detect any protein in VASP−/− animals (Fig. 2). These results were confirmed by Northern blot analysis of poly(A)$^+$ RNA isolated from spleen and large intestine that detected only *VASP* mRNA in wild-type animals but no full-length or truncated transcripts in samples from knockout mice (Fig. 3).

VASP−/− mice were macroscopically indistinguishable from wild-type animals. Heterozygous and homozygous animals were fertile and produced normal litter sizes. Crosses of heterozygotes obtained from one male chimera showed normal Mendelian transmission of genotypes (16 wild type and 20 homozygous animals of 74 offspring).

Morphology/Pathology of VASP-Deficient Mice. Histological analysis was performed with three VASP−/− and wild-type mice. In general, organs from both lines were morphologically indistinguishable. The only difference detected in histological analysis was a moderate hyperplasia of megakaryocytes in bone marrow and spleen of VASP-deficient mice. Scoring of 10 high-power fields in bone-marrow analysis yielded mean numbers of small, hyposegmentated megakaryocytes of 12.4 and 20 in wild-type and VASP−/− mice, respectively ($P < 0.0001$) (Fig. 4). In spleen mean numbers were 3.1 (wild type) and 5.3 (VASP−/−) ($P = 0.0003$).

Expression of Mena and VASP Binding Proteins. The wide absence of phenotypic differences between wild-type and VASP−/− mice suggested that other members of the Ena/VASP protein family might compensate for VASP function. Expression of Mena was investigated in tissues exhibiting high (platelets and lung), moderate (spleen), and very low expression of VASP (total brain) (Fig. 5*a*). Immunoblot analysis showed expression of the 88-kDa and 140-kDa Mena isoforms in brain, as reported previously (14), and 80-kDa and 88-kDa isoforms in lung. In platelets and in spleen Mena was not detectable. In all tissues investigated, the amounts of Mena were virtually identical in wild-type, heterozygous, and homozygous mice. Evl expression was investigated by Northern blot analysis. Strong expression was found in spleen, whereas it was week in brain and stomach (Fig. 5*b*). *Evl* mRNA was not detectable in heart and kidney. Likewise Mena and Evl expression levels were undistinguishable when comparing VASP−/− and wild-type mice. These results indicate that the levels of Mena and/or Evl expression were not affected by the absence of VASP.

Because VASP is a substrate for cGKI (1, 5, 6), and there is strong evidence that the physiological function of VASP is highly dependent on its interaction with and direct binding to profilin (16), zyxin (17), and vinculin (20, 21), the coordinated expression of these genes was investigated (Fig. 5). Although the amount of vinculin was identical in all animals and tissues examined, we observed marginal alterations for profilin, zyxin, and cGKI. These observations and their possible pathophysiological significance need further investigation.

Platelet Activation. Results from previous investigations of VASP function in platelets, the absence of Mena in mice platelets, and particularly the hyperplasia of megakaryocytes in VASP−/− mice suggested possible functional differences of platelets from wild-type and homozygous mice. Despite the moderate hyperplasia of megakaryocytes in bone marrow and spleen, the number of platelets in total blood and platelet-rich plasma was similar in wild-type and homozygous mice (data not shown). However, upon stimulation of platelet-rich plasma with 0.5 units/ml of thrombin for 1 min we observed a more than 2-fold higher surface expression of P-selectin and fibrinogen binding in VASP-deficient platelets in comparison to wild type (Fig. 6). To exclude that an increased activation of VASP−/− platelets might be the consequence of a higher number of fibrinogen receptors in the membrane, the amount of the integrin $\alpha_{IIb}\beta_3$ chain was determined by flow cytometry using the anti-mouse CD41 antibody. The level of the $\alpha_{IIb}\beta_3$ chain was similar in platelets from wild-type and homozygous animals (not shown).

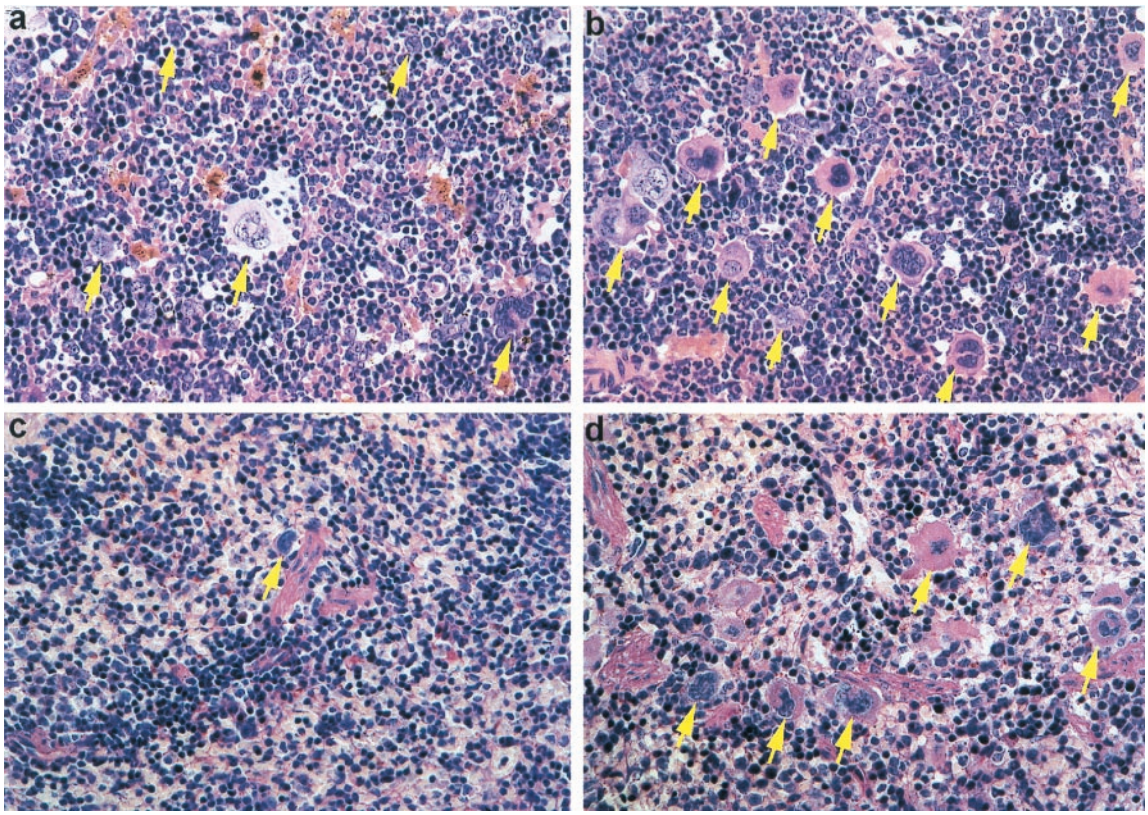

FIG. 4. Histopathology of bone marrow (*a* and *b*) and spleen (*c* and *d*) of wild-type (*a* and *c*) and VASP−/− (*b* and *d*) mice. This morphological analysis shows hyperplasia of megakaryocytopoesis in VASP−/− mice (*b* and *d*) as compared with the normocellular megakaryocytopoesis in wild-type mice (*a* and *c*). Arrows indicate megakaryocytes. Original magnification: ×150.

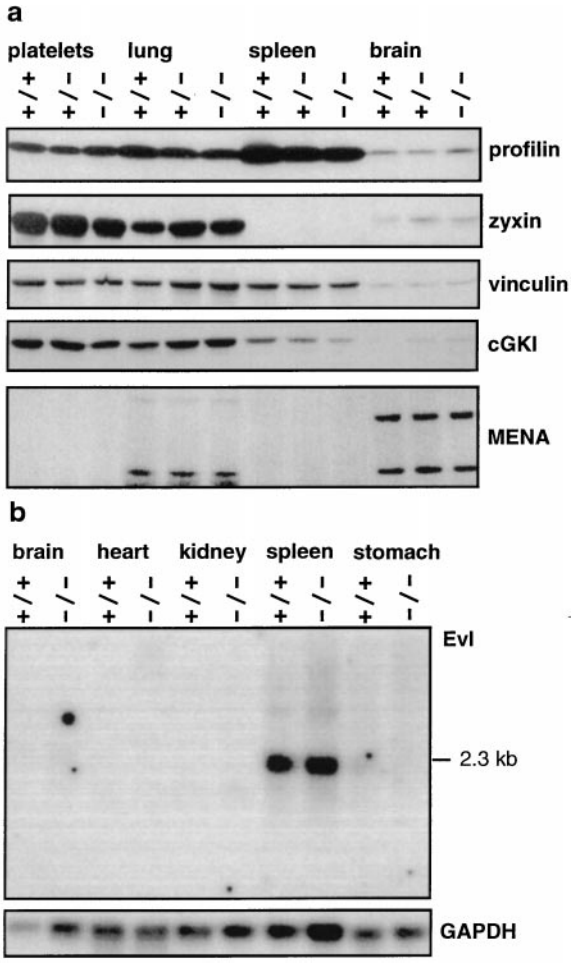

FIG. 5. Expression of Mena, Evl, profilin, zyxin, vinculin, and cGKI in platelets and selected tissues from wild-type, VASP+/−, and VASP−/− mice. (*a*) Immunoblot analysis. Whole-cell and tissue extracts (30 μg protein) were separated, blotted, and labeled as described in *Materials and Methods*. Equal protein loading was controled by Ponceau staining. Profilin, 12–15 kDa; zyxin, 83 kDa; vinculin, 117 kDa; cGKI, 74 kDa; Mena in brain, 88 kDa and 140 kDa; and Mena in lung, 80 kDa and 88 kDa. (*b*) Northern blot analysis of Evl expression. Poly(A)$^+$ RNA (3 μg) were loaded per lane, as described in *Materials and Methods*. The blot was hybridized with a mouse *Evl* cDNA probe.

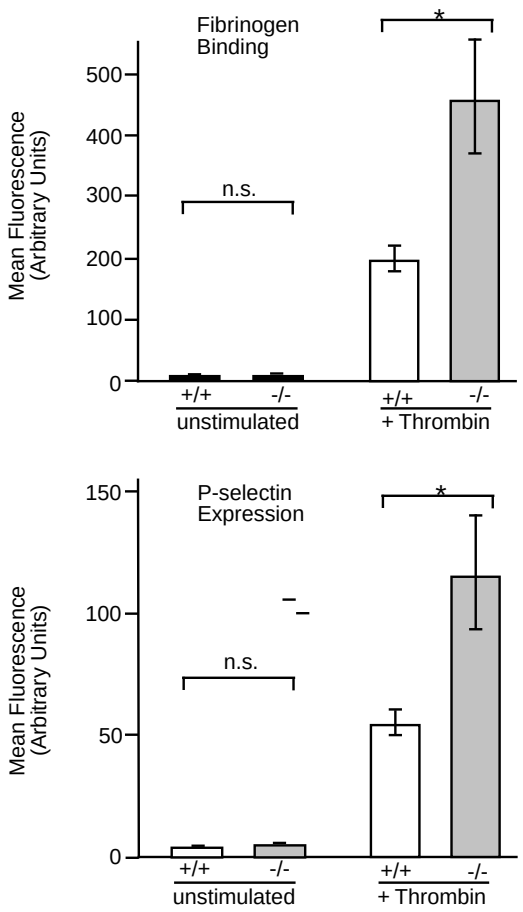

FIG. 6. Flow cytometry analysis of thrombin-induced activation of platelets obtained from wild-type (+/+) or VASP−/− mice. Acid-citric acid-dextrose anticoagulated platelet-rich plasma of wild-type (open bars), or VASP−/− (gray bars) mice was incubated with 0.5 units/ml thrombin for 1 min and analyzed for fibrinogen binding (*Upper*) or P-selectin expression (*Lower*) by flow cytometry as described in *Materials and Methods*. Histograms show mean fluorescence, and the data represent means ± SEM of three independent experiments.

Platelet activation and aggregation is strongly inhibited by cAMP- and cGMP-elevating agents and correlates with VASP phosphorylation at Ser-157 (2, 8). To investigate a possible role of VASP in this process, platelet-rich plasma was incubated in the presence of 3 μM prostaglandin E_1 for 3 min before thrombin activation. Under these conditions fibrinogen binding and P-selectin expression, as analyzed by flow cytometry and platelet aggregation, was completely inhibited in platelets from wild-type and homozygous animals (data not shown).

DISCUSSION

Targeted disruption of the murine *VASP* gene was performed to obtain information about the physiological role of this protein. In wild-type mice, VASP was expressed in most tissues and cell types. High expression levels were detected in platelets and in tissues that are rich in smooth muscle cells, including lung, stomach, large intestine, and vascular vessel walls. The strong evolutionary sequence conservation of the VASP gene and protein (11, 13), and available cell biological information, including its role in *Listeria* motility (23, 24), had indicated that VASP might have essential cellular functions. However, initial analyses of VASP-deficient mice revealed moderate hyperplasia of megakaryocytes in bone marrow and spleen and increased platelet activation, but otherwise VASP-deficient mice are phenotypically indistinguishable from wild-type mice. The limited phenotypic differences were considered to derive from functional compensation of VASP by other proteins from the Ena/VASP protein family. This hypothesis was particularly attractive because human VASP itself recently has been shown to rescue the lethal phenotype in *Drosophila* Ena null mutants (15). Therefore, expression of Mena and Evl was compared in wild-type and VASP-deficient mice. However, in all tissues examined we found no differences in expression levels. Compensation effects were expected to be most likely in phenotypically unaffected tissues with high VASP contents, e.g., lung, but in those tissues either Mena or Evl also were expressed in wild type. It is possible, therefore, that compensation of VASP function does not require an increase in expression of the other members of this protein family. The phenotypic differences observed between VASP-deficient and wild-type mice were restricted to platelets and their precursor cells only. VASP deficiency may have a measurable impact in these cells because they express high amounts of VASP but no detectable levels of Mena in either VASP+/+ or VASP−/− mice. Thus compensation of VASP function by Mena is excluded in this cell type. To evaluate the ability of Evl to compensate for VASP function needs further investigation and depends on whether Evl interacts with the same cytoskeletal proteins as VASP and Mena.

Thrombin-induced surface expression of P-selectin and fibrinogen binding to the glycoprotein $\alpha_{IIb}\beta_3$ are hallmarks of platelet

activation that results in aggregation (25, 30). As shown by FACS analysis both were clearly enhanced in VASP-deficient platelets in comparison to wild-type platelets. Enhanced fibrinogen binding was not caused by a higher number of fibrinogen receptors in VASP-deficient platelets because flow cytometry analysis using the anti-mouse CD41 antibody demonstrated similar levels of α_{IIb} proteins in platelets from wild-type and homozygous animals. Although there are still major gaps in our understanding of integrin activation and signaling, evidence indicates a prominent role of G protein-coupled actin polymerization and cytoskeletal reorganization in the process of $\alpha_{IIb}\beta_3$ activation (25). Our present observation of enhanced $\alpha_{IIb}\beta_3$ activation in VASP-deficient platelets indicates that VASP exhibits a regulatory function in thrombin-induced signal transduction pathways, and it supports the hypothesis that VASP has an inhibitory role in the process of integrin activation. However, we cannot rule out a more complex, perhaps even bimodal, functional role of VASP that could be affected by the level of VASP expression in different cell types, subcellular localization, and phosphorylation state.

Platelet activation and aggregation is strongly inhibited by cAMP- and cGMP elevating agents. Because VASP phosphorylation correlates with the fibrinogen receptor inhibition (2, 8) it was unexpected that preincubation with the cAMP-elevating prostaglandin E_1 completely prevented thrombin-induced fibrinogen binding and P-selectin expression, as well as platelet aggregation, not only in platelets from wild-type but also from knockout animals. These results demonstrate that VASP is not essential for cyclic nucleotide-mediated inhibition of thrombin-induced platelet activation and aggregation. A likely VASP-independent mechanism of platelet inhibition by cyclic nucleotides and cyclic nucleotide-dependent protein kinases is the inhibition of thrombin-induced phospholipase C activation and calcium transients (31, 32). However, VASP and cyclic nucleotide-evoked VASP phosphorylation may contribute to the inhibition of platelet activation/aggregation when transient and weak cyclic nucleotide-elevating stimuli, reflecting physiological conditions, are used. Interestingly, preliminary experiments indicated that the inhibition of platelet aggregation by low concentrations of cell-membrane permeable cyclic nucleotide analogs was impaired in VASP-deficient mice when compared with wild-type platelets. Clearly, further work with VASP deficient mice and platelets is required to understand and elucidate the regulatory role of VASP in integrin activation and signaling.

As far as directly comparable, our data agree with a recent study (33) that also reported the generation of VASP-deficient mice, which appeared after our paper had been submitted. Platelets of these mice presented with enhanced collagen-induced activation and impaired cyclic nucleotide-mediated inhibition. Interestingly, like VASP$-/-$ mice, Mena-deficient mice are viable and fertile, but exhibit a relatively mild neuronal phenotype, including impaired neurulation, decussation of the corpus callosum, and hippocampal commissure formation (34). The observed megakaryocyte hyperplasia in VASP-deficient mice suggested that the enhanced thrombin-induced platelet activation is of *in vivo* relevance. An enhanced activation and subsequent sequestration/scavenging of activated platelets is known to be compensated by megakaryocyte hyperplasia and increased platelet generation (35). VASP-deficient mice therefore could provide an interesting model systems for the analysis of diseases in which enhanced platelet activation is thought to play a major role (36), i.e., advanced arteriosclerosis, acute coronary/vascular syndromes, and inflammatory vascular diseases.

This article is dedicated to Kurt Kochsiek, professor emeritus of internal medicine, in gratitude for his long-standing support. We thank Matthias Reinhard for the affinity-purified VASP polyclonal antibody. The help of Ulrike Schwarz and Petra Hönig-Liedl in our FACS experiments and platelet function tests is also gratefully acknowledged. This work was supported by the Deutsche Forschungsgemeinschaft.

1. Waldmann, R., Nieberding, M. & Walter, U. (1987) *Eur. J. Biochem.* **167,** 441–448.
2. Halbrugge, M. & Walter, U. (1989) *Eur. J. Biochem.* **185,** 41–50.
3. Halbrugge, M., Friedrich, C., Eigenthaler, M., Schanzenbacher, P. & Walter, U. (1990) *J. Biol. Chem.* **265,** 3088–3093.
4. Eigenthaler, M., Nolte, C., Halbrugge, M. & Walter, U. (1992) *Eur. J. Biochem.* **205,** 471–481.
5. Butt, E., Abel, K., Krieger, M., Palm, D., Hoppe, V., Hoppe, J. & Walter, U. (1994) *J. Biol. Chem.* **269,** 14509–14517.
6. Smolenski, A., Bachmann, C., Reinhard, K., Honig-Liedl, P., Jarchau, T., Hoschuetzky, H. & Walter, U. (1998) *J. Biol. Chem.* **273,** 20029–20035.
7. Abel, K., Mieskes, G. & Walter, U. (1995) *FEBS Lett.* **370,** 184–188.
8. Horstrup, K., Jablonka, B., Honig-Liedl, P., Just, M., Kochsiek, K. & Walter, U. (1994) *Eur. J. Biochem.* **225,** 21–27.
9. Reinhard, M., Halbrugge, M., Scheer, U., Wiegand, C., Jockusch, B. M. & Walter, U. (1992) *EMBO J.* **11,** 2063–2070.
10. Reinhard, M., Jarchau, T., Reinhard, K. & Walter, U. (1999) in *Guidebook to the Cytoskeletal and Motor Proteins*, eds. Kreis, T. & Vale, R. (Oxford Univ. Press, Oxford), pp. 168–171.
11. Haffner, C., Jarchau, T., Reinhard, M., Hoppe, J., Lohmann, S. M. & Walter, U. (1995) *EMBO J.* **14,** 19–27.
12. Gertler, F. B., Comer, A. R., Juang, J. L., Ahern, S. M., Clark, M. J., Liebl, E. C. & Hoffmann, F. M. (1995) *Genes Dev.* **9,** 521–533.
13. Zimmer, M., Fink, T., Fischer, L., Hauser, W., Scherer, K., Lichter, P. & Walter, U. (1996) *Genomics* **36,** 227–233.
14. Gertler, F. B., Niebuhr, K., Reinhard, M., Wehland, J. & Soriano, P. (1996) *Cell* **87,** 227–239.
15. Ahern-Djamali, S. M., Comer, A. R., Bachmann, C., Kastenmeier, A. S., Reddy, S. K., Beckerle, M. C., Walter, U. & Hoffmann, F. M. (1998) *Mol. Biol. Cell.* **9,** 2157–2171.
16. Reinhard, M., Giehl, K., Abel, K., Haffner, C., Jarchau, T., Hoppe, V., Jockusch, B. M. & Walter, U. (1995) *EMBO J.* **14,** 1583–1589.
17. Reinhard, M., Jouvenal, K., Tripier, D. & Walter, U. (1995) *Proc. Natl. Acad. Sci. USA* **92,** 7956–7960.
18. Niebuhr, K., Ebel, F., Frank, R., Reinhard, M., Domann, E., Carl, U. D., Walter, U., Gertler, F. B., Wehland, J. & Chakraborty, T. (1997) *EMBO J.* **16,** 5433–5444.
19. Chakraborty, T., Ebel, F., Domann, E., Niebuhr, K., Gerstel, B., Pistor, S., Temm-Grove, C. J., Jockusch, B. M., Reinhard, M., Walter, U., *et al.* (1995) *EMBO J.* **14,** 1314–1321.
20. Reinhard, M., Rudiger, M., Jockusch, B. M. & Walter, U. (1996) *FEBS Lett.* **399,** 103–107.
21. Brindle, N. P., Holt, M. R., Davies, J. E., Price, C. J. & Critchley, D. R. (1996) *Biochem. J.* **318,** 753–757.
22. Kang, F., Laine, R. O., Bubb, M. R., Southwick, F. S. & Purich, D. L. (1997) *Biochemistry* **36,** 8384–8392.
23. Dramsi, S. & Cossart, P. (1998) *Annu. Rev. Cell Dev. Biol.* **14,** 137–166.
24. Beckerle, M. C. (1998) *Cell* **95,** 741–748.
25. Shattil, S. J., Kashiwagi, H. & Pampori, N. (1998) *Blood* **91,** 2645–2657.
26. Rudnicki, M. A., Braun, T., Hinuma, S. & Jaenisch, R. (1992) *Cell* **71,** 383–390.
27. Sambrook, J., Fritsch, E. F. & Maniatis, T. (1989) *Molecular Cloning: A Laboratory Manual* (Cold Spring Harbor Lab. Press, Plainview, NY), 2nd Ed.
28. Church, G. M. & Gilbert, W. (1984) *Proc. Natl. Acad. Sci. USA* **81,** 1991–1995.
29. Gambaryan, S., Hausler, C., Markert, T., Pohler, D., Jarchau, T., Walter, U., Haase, W., Kurtz, A. & Lohmann, S. M. (1996) *J. Clin. Invest.* **98,** 662–670.
30. Berman, C. L., Yeo, E. L., Wencel-Drake, J. D., Furie, B. C., Ginsberg, M. H. & Furie, B. (1986) *J. Clin. Invest.* **78,** 130–137.
31. Meinecke, M., Geiger, J., Butt, E., Sandberg, M., Jahnsen, T., Chakraborty, T., Walter, U., Jarchau, T. & Lohmann, S. M. (1994) *Mol. Pharmacol.* **46,** 283–290.
32. Schmidt, H. H., Lohmann, S. M. & Walter, U. (1993) *Biochim. Biophys. Acta* **1178,** 153–175.
33. Aszodi, A., Pfeifer, A., Ahmad, M., Glauner, M., Zhou, X. H., Ny, L., Andersson, K.-E., Kehrel, B., Offermanns, S. & Fassler, R. (1999) *EMBO J.* **18,** 37–48.
34. Lanier, L. M., Gates, M. A., Witke, W., Menzies, A. S., Wehman, A. M., Macklis, J. D., Kwiatkowski, D., Soriano, P. & Gertler, F. B. (1999) *Neuron* **22,** 313–325.
35. Nieuwenhuis, H. K. & Sixma, J. J. (1992) *N. Engl. J. Med.* **327,** 1812–1813.
36. Handin, R. I. (1996) *N. Engl. J. Med.* **334,** 1126–1127.